RESEARCH ARTICLE | JULY 27 2020

# Interpolating $QCD_2$ between the instant and front forms of relativistic dynamics

Bailing Ma; Chueng-Ryong Ji



*AIP Conf. Proc.* 2249, 030009 (2020)
https://doi.org/10.1063/5.0008605



# Interpolating $QCD_2$ between the Instant and Front Forms of Relativistic Dynamics

Bailing Ma[a)] and Chueng-Ryong Ji[b)]

*Department of Physics, North Carolina State University, Box 8202, Raleigh, NC 27695-8202, USA*

[a)] *bma4@ncsu.edu*
[b)] *Corresponding author: crji@ncsu.edu*

**Abstract.** The two-dimensional quantum chromodynamics ($QCD_2$) in the limit of infinite number of colors, known as 't Hooft model, was originally formulated in the Light Front Dynamics (LFD). The theory is exactly solvable, while still bearing some resemblance to the four-dimensional real world QCD in aspects such as confinement and mass gap, as well as the spontaneous breaking of chiral symmetry. The work in the Instant Form Dynamics (IFD) was done in 1978 by Bars and Green. The quark-antiquark bound state equation was derived and solved in each of the two forms, i.e., 't Hooft equation and Bars-Green equations, respectively, and they give the same discrete meson mass spectrum independent of the quantization form as expected. Introducing an interpolation angle parameter $\delta$, in this work, we link the two distinct forms of dynamics, IFD and LFD, by letting the space-time axes rotate from the ordinary equal-time form $\{t,x\}$ to the light front form $\{x^+,x^-\}$, as $\delta$ varies from 0 to $\pi/4$. We unify the 't Hooft and Bars-Green equations into one formula, and by numerically solving it we confirm the independence of the meson mass spectra on the interpolation angle $\delta$. We note that the quark condensate is quantization angle independent. This indicates a non-trivial vacuum structure even in the light-front form.

## INTRODUCTION

The two-dimensional quantum chromodynamics ($QCD_2$) has served as a theoretical laboratory for the study of strong interactions since 't Hooft's seminal paper in 1974 [1]. In that paper, by solving this model, he demonstrated the power of $1/N$ expansion [2], which was then widely studied (e.g. by Witten [3]), and is believed to be equivalent to the topological expansion in string theory, with $1/N$ being the string coupling constant. Under the large $N$ approximation, non-planar diagrams are negligible. Thus, only rainbow diagrams need to be summed over for the quark self mass. In addition, the gluon self-couplings are absent, at least in a certain gauge. Being a 1+1 dimensional theory, 't Hooft model exhibits the confinement, which is simply due to the Coulomb potential becoming linear when restricted to one spatial dimension, unlike in four-dimensional gauge theories, where it must arise from non-perturbative aspects. Nevertheless, the model remains of interest as a nontrivial, but solvable quantum field theory of confinement.

The 't Hooft model was originally formulated using the Light Front Dynamics (LFD). Later, Bars and Green re-derived it in the traditional Instant Form Dynamcis (IFD) [4]. While an analytic solution for the bound state equation was not presented in Bars and Green's work, the Bars-Green equation was solved numerically in the rest frame of the meson [5] as well as in moving frames [6]. The obtained meson spectrum in any frame with arbitrary center-of-mass momentum is shown to agree with the one solved by 't Hooft in LFD.

The three forms of Hamiltonian dynamics including the IFD, LFD, and the point form were originally proposed by Dirac in 1949 [7]. However, only in recent years people started to connect the two most popular forms, i.e., IFD and LFD [8]. The LFD has the advantage of having seven kinematical operators among the ten Poincarè operators, while the IFD and point form both have only six. More kinematical operators mean having more symmetry properties, and correspondingly the large efforts in dynamics can be saved. Through the interpolation method, it can be made clear how the longitudinal boost operation becomes kinematical when the dynamical form approaches to the LFD [9]. The issue of zero modes in the LFD can also be examined more explicitly. In our previous works, we have applied the interpolation method to the scattering amplitude of two scalar particles [10], the electromagnetic gauge field [11], as well as the helicity spinors [12] in the theory of Quantum Electrodynamics (QED). We have established the interpolating QED theory between the IFD and LFD [13]. By studying the interpolation form of the fermion propagator under the limit to both IFD and LFD, we emphasize the importance of zero mode contribution in the light-front, i.e., it gives rise to the fermion instantaneous propagator, which cannot be ignored if an equivalence to the covariant theory is to be obtained.

In this work, we apply the interpolation idea to the 1+1 dimensional QCD. We give the quark self-energy equation in $QCD_2(N \to \infty)$ in an arbitrary quantization form interpolating between the IFD and LFD, and solve the interpolating equation numerically. We unify the 't Hooft bound state equation and Bars-Green equation into one formula, which reproduces each corresponding equation when the limit to LFD or IFD is taken. We numerically confirm the in-

*Proceedings of the 15th International Conference on Meson-Nucleon Physics and the Structure of the Nucleon*
AIP Conf. Proc. 2249, 030009-1–030009-7; https://doi.org/10.1063/5.0008605
Published by AIP Publishing. 978-0-7354-2008-3/$30.00

dependence of meson spectrum regardless of the interpolation angle. We also verify that there is a non-trivial vacuum condensate, i.e., $< \bar{\psi}\psi > \neq 0$ as we take the light-front limit, as Refs. [14, 15, 16] have noted. In this paper, we will be focusing mainly in the weak coupling regime of $QCD_2$, i.e. $m >> g$. When taking $N \to \infty$, the 't Hooft coupling $\lambda \sim g^2 N$ is kept constant, where $g$ is the coupling constant of the theory, which means that $g \to 0$, i.e., theory is in the weak coupling regime. It is known that there are at least two phases in $QCD_2$ [17], and the strong coupling regime can be studied by the bosonization method [18]. Naive extension of the 't Hooft model to the strong coupling regime ($m << g$) will cause problems, and we keep $m >> g$ when taking the chiral limit by letting $N \to \infty$ first before letting $m \to 0$.

## MASS GAP EQUATION IN INTERPOLATION FORM

The 't Hooft model is particularly simple and solvable not only because of its $1+1$ dimensionality, but also thanks to the usage of light-front quantization form, let alone the power of large $N$ approximation. In light-front form of dynamics, the two-dimensional space-time coordinates are defined as

$$x^{\pm} = \frac{1}{\sqrt{2}}\left(x^0 \pm x^1\right), \tag{1}$$

where $x^+$ is defined as the light-front time variable, while $x^-$ is the corresponding space variable.

The momentum variables with lower-indices are conjugate to positions, i.e.

$$p_+ = \frac{1}{\sqrt{2}}\left(p_0 + p_1\right) = \frac{1}{\sqrt{2}}\left(p^0 - p^1\right) = p^-, \tag{2}$$

$$p_- = \frac{1}{\sqrt{2}}\left(p_0 - p_1\right) = \frac{1}{\sqrt{2}}\left(p^0 + p^1\right) = p^+, \tag{3}$$

where $p^-$ is the light-front energy, and $p^+$ is the light-front longitudinal momentum. Notice that the light-front metric is completely off-diagonal. Due to the special summation convention $p^2 = 2p^+p^-$, energy-momentum relation for on-mass-shell particle is rational in the LFD

$$p^- = \frac{m^2}{2p^+}. \tag{4}$$

Also, the sign of momentum $p^+$ is correlated with the energy $p^-$. This is in contrast to the IFD, where the relationship is irrational $p^0 = \sqrt{m^2 + (p^1)^2}$, and the momentum $p^1$ can take both signs.

In order to link the two distinctive forms of dynamics, and to take advantages of both the familiarity of the IFD and some of the simplicity of the LFD, we introduce the interpolation form between the IFD and LFD. We rotate the space-time axes of the instant form by a continuous parameter $\delta$, i.e.

$$\begin{bmatrix} x^{\hat{+}} \\ x^{\hat{-}} \end{bmatrix} = \begin{bmatrix} \cos\delta & \sin\delta \\ \sin\delta & -\cos\delta \end{bmatrix} \begin{bmatrix} x^0 \\ x^1 \end{bmatrix}. \tag{5}$$

The interpolation angle, $\delta$, runs from $0^\circ$ to $45^\circ$. The lower index variables $x_{\hat{+}}$ and $x_{\hat{-}}$ are related to the upper ones by $x_{\hat{+}} = g_{\hat{+}\hat{+}}x^{\hat{+}} + g_{\hat{+}\hat{-}}x^{\hat{-}} = \mathbb{C}x^{\hat{+}} + \mathbb{S}x^{\hat{-}}$ and $x_{\hat{-}} = g_{\hat{-}\hat{+}}x^{\hat{+}} + g_{\hat{-}\hat{-}}x^{\hat{-}} = \mathbb{S}x^{\hat{+}} - \mathbb{C}x^{\hat{-}}$, where the short-hand notations are defined as $\mathbb{C} = \cos 2\delta$ and $\mathbb{S} = \sin 2\delta$. All the indices with the hat-notation signify the variables with the interpolation angle $\delta$, and when $\delta = \frac{\pi}{4}$ specifically, the variables coincide with those in LFD without the hat-notation.

When $\delta = 0$, we recover the ordinary instant form dynamics, with the space-time coordinate system being $\{x^0, -x^1\}$, and when $\delta = \frac{\pi}{4}$, we are in the light front form with coordinates $\{x^+, x^-\}$. By varying the parameter $\delta$ and studying the limiting behavior when $\delta$ approaches $\frac{\pi}{4}$, we can trace the fates of symmetry properties, Poincare operators, vacuum structure, as well as calculations of physical processes such as scattering amplitudes [9, 10, 11, 12, 13]. We clear up the prevailing confusion of a particular reference frame (a system of space time axes moving with certain velocity with respect to the laboratory frame) with a quantization form (where the definition of the "time" variable is changed). In particular, we remove the confusion of the Infinite Momentum Frame (IMF) in equal-time

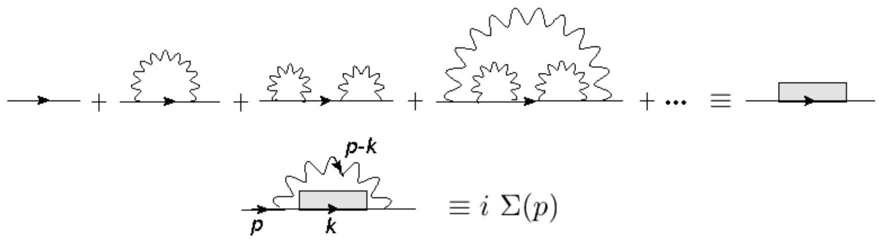


FIGURE 1: Self-energy equation

dynamics with the LFD. Both formulations, IMF and LFD, have the property that the contributions of backward propagating time-ordered diagrams tend to vanish. However, in IMF the time-ordering is done with ordinary time, while in LFD the ordering is by light-front time. The LFD has the property of boost invariance, i.e., the amplitude of a time-ordered diagram does not change no matter what reference frame is taken, while the IMF result is only valid when the particles involved are boosted to the infinite momentum. We emphasize that IMF and LFD are distinctively different from each other.

By using the interpolation form, we are also able to clarify and emphasize the role of zero modes in the LFD. Although vacuum is trivial for all $p^+ > 0$, the $p^+ = 0$ mode has to be considered because that is where all the vacuum condensations pile up. By making $\frac{\pi}{4} - \delta$ small but non-zero, we can have control over some singularities caused by $p^+ = 0$ in the light-front.

The Lagrangian of $1+1$ dimensional QCD theory in the interpolation form is

$$\mathscr{L} = -\frac{1}{4} F^a_{\hat{\mu}\hat{\nu}} F^{\hat{\mu}\hat{\nu}a} + \bar{\psi}(i\gamma^{\hat{\mu}} D_{\hat{\mu}} - m)\psi, \tag{6}$$

where

$$D_{\hat{\mu}} = \partial_{\hat{\mu}} - igA^a_{\hat{\mu}} t_a \tag{7}$$

and

$$F^a_{\hat{\mu}\hat{\nu}} = \partial_{\hat{\mu}} A^a_{\hat{\nu}} - \partial_{\hat{\nu}} A^a_{\hat{\mu}} + g f^{abc} A^b_{\hat{\mu}} A^c_{\hat{\nu}}. \tag{8}$$

The 't Hooft limit is defined as

$$N \to \infty;\ g^2 N \text{ fixed}, \tag{9}$$

where the 't Hooft coupling is given by

$$\lambda = \frac{g^2 N}{4\pi}. \tag{10}$$

Similar to the work of Bars and Green [4] in instant form dynamics, we write down the Dyson-Schwinger equation for the diagram shown in Fig. 1, where in the kernel, all possible diagrams that is planar are summed over:

$$\Sigma(p_{\hat{-}}) = i\frac{\lambda}{2\pi} \int \frac{dk_{\hat{-}} dk_{\hat{+}}}{\left(p_{\hat{-}} - k_{\hat{-}}\right)^2} \gamma^{\hat{+}} \frac{1}{\not{k} - m - \Sigma(k_{\hat{-}}) + i\varepsilon} \gamma^{\hat{+}}. \tag{11}$$

We write the quark self interaction as

$$\Sigma(p_{\hat{-}}) = \sqrt{\mathbb{C}} A(p_{\hat{-}}) + \gamma_{\hat{-}} B(p_{\hat{-}}). \tag{12}$$

In this way, the mass gap equation for a dressed quark in interpolation form is obtained as follows

$$\frac{p_{\hat{-}}}{\mathbb{C}} \cos\theta(p_{\hat{-}}) - \frac{m}{\sqrt{\mathbb{C}}} \sin\theta(p_{\hat{-}}) = \frac{\lambda}{2} \int \frac{dk_{\hat{-}}}{(p_{\hat{-}} - k_{\hat{-}})^2} \sin\left(\theta(p_{\hat{-}}) - \theta(k_{\hat{-}})\right), \tag{13a}$$

$$E(p_{\hat{-}}) = p_{\hat{-}} \sin\theta(p_{\hat{-}}) + \sqrt{\mathbb{C}} m \cos\theta(p_{\hat{-}}) + \frac{\lambda}{2} \int \frac{dk_{\hat{-}}}{(p_{\hat{-}} - k_{\hat{-}})^2} \cos\left(\theta(p_{\hat{-}}) - \theta(k_{\hat{-}})\right), \tag{13b}$$

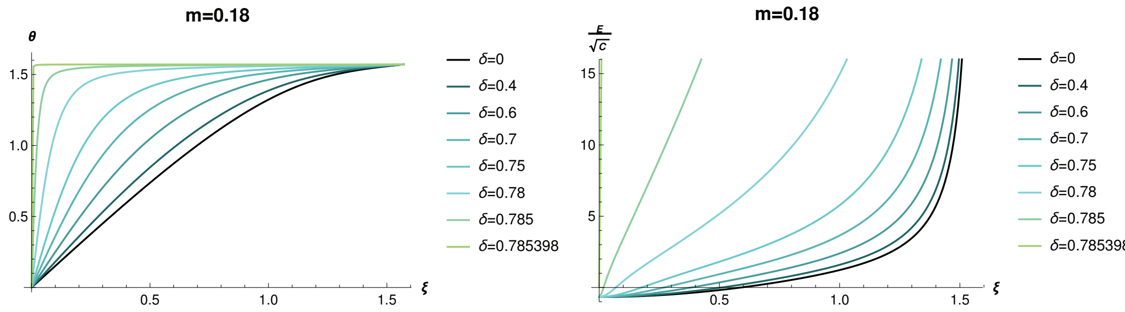


(a) (b)

FIGURE 2: Solutions of (a) $\theta$ (b) $E$ in several different interpolating forms for quark mass value $m = 0.18$. All quantities are in proper units of $\sqrt{2\lambda}$. $\xi$ comes from the variable change $p_{\hat{-}} = \tan\xi$. $\theta$ is an odd function of $p_{\hat{-}}$, and $E$ is an even function of $p_{\hat{-}}$, we only plot for positive $p_{\hat{-}}$.

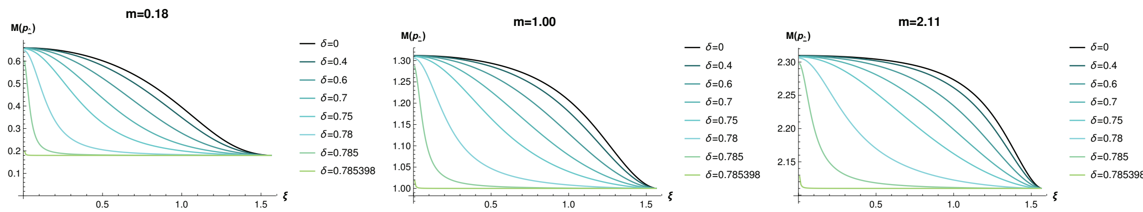


(a) (b) (c)

FIGURE 3: Constituent mass as a function of $p_{\hat{-}}$ for (a) $m = 0.18$ (b) $m = 1.00$ and (c) $m = 2.11$. All quantities are in proper units of $\sqrt{2\lambda}$.



in which $E(p_{\hat{-}})$ and $\theta(p_{\hat{-}})$ are related to $A(p_{\hat{-}})$ and $B(p_{\hat{-}})$ in Eq. (12) as

$$E(p_{\hat{-}})\cos\theta(p_{\hat{-}}) = \sqrt{\mathbb{C}}m + \mathbb{C}A(p_{\hat{-}}), \tag{14a}$$
$$E(p_{\hat{-}})\sin\theta(p_{\hat{-}}) = p_{\hat{-}} + \mathbb{C}B(p_{\hat{-}}). \tag{14b}$$

The gap equation, Eq. (13), is numerically solved following the numerical method mentioned in Ref. [5].

In actual computations, the integral is understood with the principal value prescription

$$\int \frac{dy}{(x-y)^2} f(y) \to \int \frac{dy}{(x-y)^2}\left[f(y) - f(x) - (y-x)\frac{df(x)}{dx}\right]$$
$$\equiv ⨍ \frac{dy}{(x-y)^2} f(y). \tag{15}$$

In Fig. 2a, we show the solutions of $\theta(p_{\hat{-}})$ by numerically solving Eq. (13a), for several different values of the interpolation angle. As $\delta$ gets closer to the exact light-front value, $\delta = \frac{\pi}{4}$, the solution of $\theta$ approaches to a step-function shape. In Fig. 2b, we show the solutions of $E(p_{\hat{-}})$ from Eq. (13b). For convenience of the plot, we divide it by $\sqrt{\mathbb{C}}$. As mentioned in Ref. [5], as well as in Ref. [4], the quantity $E$, which becomes the self energy of the quark in IFD, is not positive definite as can be seen from the figure. When $\delta = 0$, i.e., the curves colored black in both figures agree with the ones shown in Ref. [5]. As for $\delta \to \frac{\pi}{4}$, our solutions in light green color agree with the full quark propagator given in Ref. [1], which, written under our notation, is $S(p) = \frac{p_-}{2p_+p_- - m^2 + 2\lambda}$.

Fig. 3 shows the constituent mass as a function of the interpolating longitudinal momentum variable. Using the constituent mass function, the full quark propagator can be written as $S(p) = \frac{F(p)}{\not{p} - M(p)}$, where $F(p)$ is the wavefunction renormalization factor, which is plotted in Fig. 4. The black curves in Fig. 3 (i.e. the instant form solution $M(p^1)$), correspond in fact to the Euclidean mass function in the Dyson-Schwinger formalism. When we take $p^0 = 0$, the

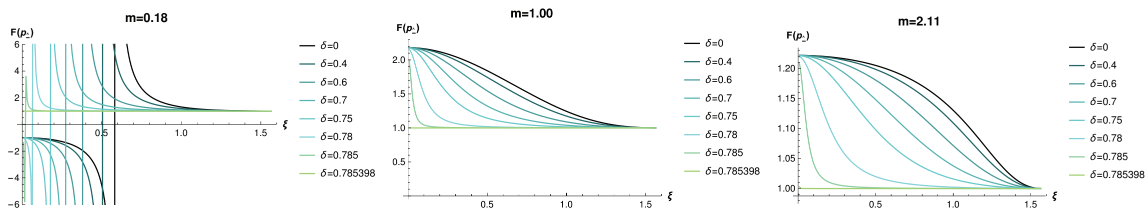


(a) (b) (c)

FIGURE 4: Wavefunction renormalization as a function of $p_{\hat{-}}$ for (a) $m = 0.18$ (b) $m = 1.00$ and (c) $m = 2.11$. All quantities are in proper units of $\sqrt{2\lambda}$.

TABLE I: Numerical calculation of quark condensate

| $\delta$ | number of computational grid points | $< \bar{\psi}\psi >_{m=0} /N$ |
|---|---|---|
| 0 | 200 | $-0.285$ |
| | 600 | $-0.288$ |
| 0.4 | 200 | $-0.285$ |
| | 600 | $-0.287$ |
| 0.6 | 200 | $-0.285$ |
| | 600 | $-0.287$ |
| 0.7 | 200 | $-0.284$ |
| | 600 | $-0.287$ |
| 0.75 | 200 | $-0.282$ |
| | 600 | $-0.286$ |
| 0.78 | 200 | $-0.297$ |
| | 600 | $-0.291$ |
| 0.785 | 1000 | $-0.294$ |
| | 3000 | $-0.291$ |
| 0.785398 | 3000 | $-0.396$ |
| | 4600 | $-0.344$ |



Minkowski and Euclidean definitions of two-momentum squared $p^2$ coincide. Just changing the variable of the horizontal axis back to $p^1 = \tan\xi$ and squaring it, we obtain the usual plot $M(p^2)$.

## VACUUM CONDENSATION

The quark vacuum condensation in the interpolation form is found to be (when $m = 0$)

$$< \bar{\psi}\psi >= -\frac{N}{\pi\sqrt{\mathbb{C}}}\int_0^{+\infty} dp_{\hat{-}} \cos\theta(p_{\hat{-}}). \tag{16}$$

Plugging in the solution shown in Fig. 2a, we can calculate the value of the condensate. We find a consistent value ($-0.29$) independent of what value $\delta$ is, although for $\delta$ closer to $\pi/4$, higher computational accuracy is needed to obtain the correct value. This value $-0.29$ is in agreement with the previous instant form calculation [14]. Also it matches with the numerical value of $-\frac{1}{\sqrt{12}}$, as other studies have analytically obtained using the QCD sum-rule and the operator expansion methods [15, 16]. Especially, we find that even when $\delta$ is six digits accurate to the light-front value ($\frac{\pi}{4} \approx 0.785398$), we still do not see any transition to a trivial vacuum. The result for $\delta = 0.785398$ is not as accurate as others although an already very large number of computational grid points is taken, because as we can see from the light-green solution of $\theta$ in Fig. 2a, $\cos\theta(p_{\hat{-}}) = 0$ for all $p_{\hat{-}} > 0^+$, which does not give any contribution. However, there is a contribution from the $p_{\hat{-}}$ near zero region, which is easily missed if the grid is too coarse, and that small quantity working with the $\sqrt{\mathbb{C}}$ (goes to zero when approaching to the light-front) in the denominator, gives the finite value, which we expect to be also about $-0.29$, as the trend of increasing grid points shows.

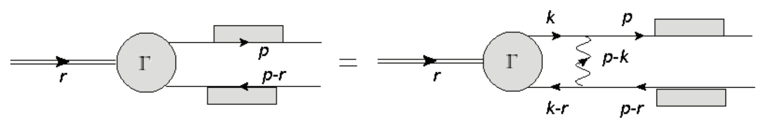


FIGURE 5: Bethe-Salpethe equation for a quark-antiquark bound state

TABLE II: Meson mass spectra

| $n$ | 0 | 1 | 2 | 3 | 4 | 5 | 6 | 7 |
|---|---|---|---|---|---|---|---|---|
| $m = 0$ | 0 | 2.43 | 3.76 | 4.81 | 5.69 | 6.46 | 7.15 | 7.79 |
| $m = 0.18$ | 0.88 | 2.74 | 4.00 | 5.00 | 5.86 | 6.61 | 7.30 | 7.92 |
| $m = 1.00$ | 2.70 | 4.16 | 5.21 | 6.09 | 6.85 | 7.54 | 8.16 | 8.75 |
| $m = 2.11$ | 4.91 | 6.17 | 7.06 | 7.83 | 8.51 | 9.13 | 9.69 | 10.23 |

## BOUND STATE EQUATION

After solving the single body Dyson-Schwinger equation, we now discuss the bound-state problem. We write down the Bethe-Salpethe equation for the diagram shown in Fig. 5, and after some derivation, we arrive at the following set of equations, where $\phi_+$ and $\phi_-$ are the two components of the mesonic wave function, representing the forward and backward motion of the quark-antiquark, respectively,

$$\left[-r^{\hat{+}} + E(xr_{\hat{-}}) + E(r_{\hat{-}} - xr_{\hat{-}})\right] r_{\hat{-}}\phi_+(r_{\hat{-}},x) = \lambda\mathbb{C}\fint \frac{dy}{(x-y)^2}\left[C(x,y,r_{\hat{-}})\phi_+(r_{\hat{-}},y) - S(x,y,r_{\hat{-}})\phi_-(r_{\hat{-}},y)\right] \tag{17a}$$

$$\left[r^{\hat{+}} + E(r_{\hat{-}} - xr_{\hat{-}}) + E(xr_{\hat{-}})\right] r_{\hat{-}}\phi_-(r_{\hat{-}},x) = \lambda\mathbb{C}\fint \frac{dy}{(x-y)^2}\left[C(x,y,r_{\hat{-}})\phi_-(r_{\hat{-}},y) - S(x,y,r_{\hat{-}})\phi_+(r_{\hat{-}},y)\right], \tag{17b}$$

where

$$C(x,y,r_{\hat{-}}) = \cos\left(\frac{\theta(xr_{\hat{-}}) - \theta(yr_{\hat{-}})}{2}\right)\cos\left(\frac{\theta(r_{\hat{-}} - xr_{\hat{-}}) - \theta(r_{\hat{-}} - yr_{\hat{-}})}{2}\right), \tag{18a}$$

$$S(x,y,r_{\hat{-}}) = \sin\left(\frac{\theta(xr_{\hat{-}}) - \theta(yr_{\hat{-}})}{2}\right)\sin\left(\frac{\theta(r_{\hat{-}} - xr_{\hat{-}}) - \theta(r_{\hat{-}} - yr_{\hat{-}})}{2}\right), \tag{18b}$$

and $x \equiv p_{\hat{-}}/r_{\hat{-}}$, $y \equiv k_{\hat{-}}/r_{\hat{-}}$.

We solved the equations following the methods of Li [5] for the meson in its rest frame, as well as more recently Jia et al. [6] in the moving frame of the meson. We find the consistent meson mass spectra for any interpolation angle and any total longitudinal momentum of the meson in agreement with the previous result obtained in instant form [5, 6], as shown in Table II, and plotted in Fig. 6. The wavefunctions are also obtained and will be presented in a separate publication [19].

## CONCLUSION

The work of 't Hooft model in instant form of dynamics is generalized to any interpolation angle between the IFD and LFD. A consistent meson mass spectra is obtained independent of not only the interpolation angle but also the choice of reference frame. The QCD vacuum is found to be non-trivial even in the light-front, and no phase transition was observed when passing from the instant form to the light-front form.

## ACKNOWLEDGMENTS

This work was supported by the U.S. Department of Energy Grant No. DE-FG02-03ER41260. This research used resources of the National Energy Research Scientific Computing Center, which is supported by the Office of Science

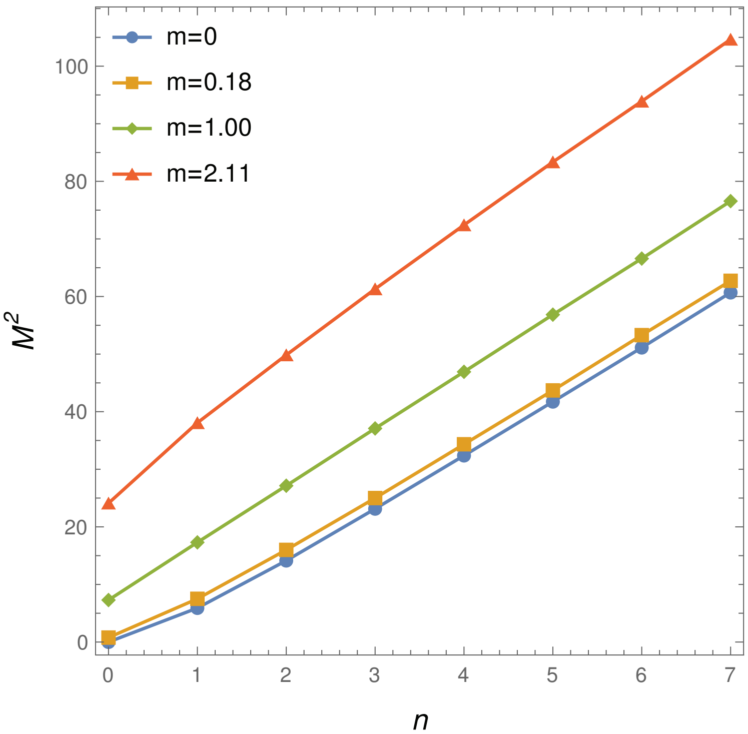


FIGURE 6: Meson mass spectra of several lowest-level states for four different quark bare mass values



of the U.S. Department of Energy under Contract No. DE-AC02-05CH11231. One of us (Bailing Ma) wishes to thank colleague Jiaxun Hou for discussions on some calculation.

## REFERENCES

1. G. 't Hooft, Nucl. Phys. **75**, 461 (1974).
2. G. 't Hooft, Nucl. Phys. **72**, 461 (1974).
3. E. Witten, Nucl. Phys. B **160**, 57 (1979).
4. I. Bars and M. B. Green, Phys. Rev. D **17**, 537 (1978).
5. M. Li, L. Wilets, and M. C. Birse, J. Phys. G: Nucl. Phys. **13**, 915 (1987).
6. Y. Jia, S. Liang, L. Li, and X. Xiong, JHEP **11**, 151 (2017).
7. P. A. M. Dirac, Rev. Mod. Phys. **21**, 392 (1949).
8. K. Hornbostel, Phys. Rev. D **45**, 3781 (1992).
9. C.-R. Ji and C. Mitchell, Phys. Rev. D **64**, 085013 (2001).
10. C.-R. Ji and A. T. Suzuki, Phys. Rev. D **87**, 065015 (2013).
11. C.-R. Ji, Z. Li, and A. T. Suzuki, Phys. Rev. D **91**, 065020 (2015).
12. Z. Li, M. An, and C.-R. Ji, Phys. Rev. D **92**, 105014 (2015).
13. C.-R. Ji, Z. Li, B. Ma, and A. T. Suzuki, Phys. Rev. D **98**, 036017 (2018).
14. M. Li, Phys. Rev. D **34**, 3888 (1986).
15. A. Zhitnitsky, Phys. Lett. B **165**, 405 (1985).
16. M. Burkardt, Phys. Rev. D **53**, 933 (1996).
17. V. Baluni, Phys. Lett. B **90**, 407 (1980).
18. P. Steinhardt, Nucl. Phys. B **176**, 100 (1980).
19. B. Ma and C.-R. Ji, In preparation.
20. Y. S. Kalashnikova and A. V. Nefed'ev, Phys.-Usp. **45**, 347 (2002).
21. C.-R. Ji, Few-Body Syst. **52**, 421–426 (2012).
22. M. E. Peskin and D. V. Schroeder, "An introduction to quantum field theory," (Addison-Wesley Publishing Company, Reading, 1997).